Electronic Supplementary Material (ESI) for Chemical Communications

Coexistence of cages and one-dimensional channels in a porous MOF with high H_2 and CH_4 uptakes

Jiandong Pang,[ab] Feilong Jiang,[a] Mingyan Wu,[a] Daqiang Yuan,[a] Kang Zhou,[ab] Jinjie Qian,[ab] Kongzhao Su,[ab] and Maochun Hong*[a]*

[a]State Key Laboratory of Structure Chemistry, Fujian Institute of Research on the Structure of Matter, Chinese Academy of Sciences, Fuzhou, Fujian, 350002, China
[b] University of the Chinese Academy of Sciences, Beijing, 100049, China

Supporting Information:

Experimental Section

Fig. S1 Two extreme conformations of obdb ligand. a) the ligand in C_2 symmetry ; b) the ligand in C_s symmetry.
Fig. S2 a) Combination of the three types of polyhedral cages viewed along *a* axis; b) Combination of the three types of polyhedral cages viewed along *c* axis; c) packing of the framework viewed along *a* axis; d) packing of the framework viewed along *c* axis.
Fig. S3. Topology of **FJI-H5** simplified both obdb ligands and the Cu_2 SBUs as 4-connected nodes.
Fig. S4. Powder X-ray diffraction (PXRD) patterns of **FJI-H5**: pattern simulated from single-crystal structure in black, experimental pattern for the as-synthesized sample in red and that for the sample after adsorption in blue.
Fig. S5. TGA curves of **FJI-H5**.
Fig. S6. Isosteric heat of H_2 adsorption at low coverage for **FJI-H5**.
Fig. S7. Isosteric heat of CH_4 adsorption at low coverage for **FJI-H5**.
Fig. S8. Isosteric heat of CO_2 adsorption at low coverage for **FJI-H5**.
Fig. S9. Sorption isotherms for CO_2, CH_4 and N_2 at 273 K of **FJI-H5**.
Fig. S10. Sorption isotherms for CO_2, CH_4 and N_2 at 283 K of **FJI-H5**.
Fig. S11. Sorption isotherms for CO_2, CH_4 and N_2 at 293 K of **FJI-H5**.
Fig. S12. IAST selectivities of CO_2 over N_2 for 15% CO_2, 85% N_2 binary mixtures in **FJI-H5** at 273K.
Fig. S13. IAST selectivities of CO_2 over CH_4 for equimolar binary mixtures in **FJI-H5** at 273 K.
Table S1. Crystal data and structure refinement for **FJI-H5**.
Table S2. H_2 adsorption data for selected MOFs at 1 atm and 77 K.

Experimental Section

Synthesis of H_4obdb:

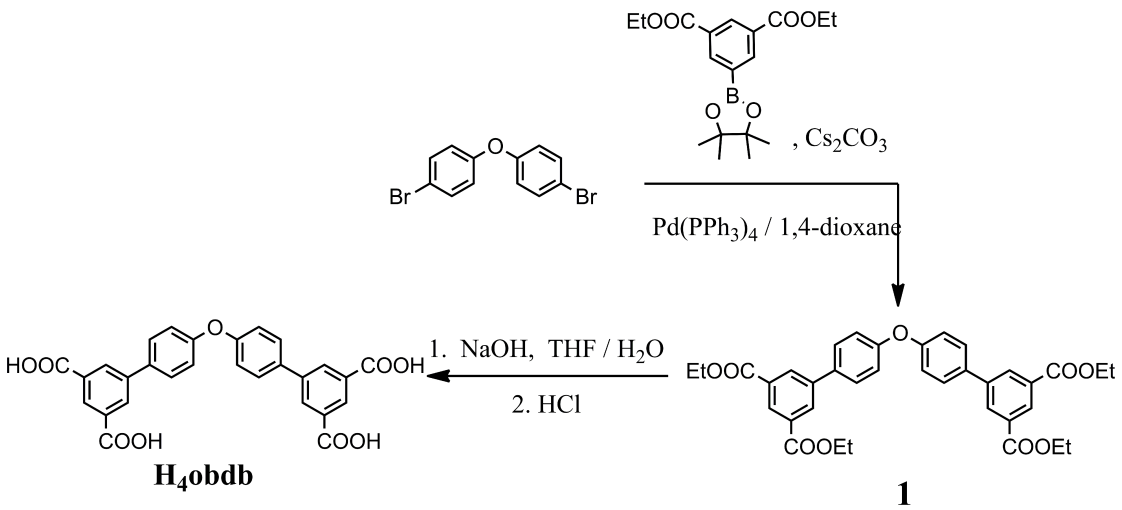

Scheme S1: *Synthesis scheme of the ligand.*

Synthesis of tetraethyl 4',4'''-oxybis([1,1'-biphenyl]-3,5-dicarboxylate) (1):
4,4'-oxybis(bromobenzene) (1.32 g, 0.004 mol), diethyl 5-(4,4,5,5-tetramethyl-1,3,2-dioxaborolan-2-yl)-1,3-benzene-dicarboxylate[1] (3.062 g, 0.0088 mol), cesium carbonate (8.07 g, 0.025 mol) and tetrakis(triphenylphosphine)palladium (0.2g, 0.0002 mol) were added to a 250-mL schlenk flask charged with stir bar. The flask was pumped under vacuum and refilled with N_2 for three times, and then 150 mL of degassed solvent of 1,4-dioxane was transferred to the system and the solution was refluxed for 48h under nitrogen atmosphere. After the reaction mixture was cooled to room temperature, the organic solvent was evaporated, and the solid was washed with water. The aqueous layer was extracted with dichloromethane (3 × 50 mL) then, and the combined organic layers were dried over magnesium sulfate and filtered. After remove the dichloromethane, the crude product was purified by column chromatography on silica gel with ethyl acetate / hexane (v/v = 1:6) to give compound **1** as a pale yellow solid. (1.83 g, 0.003 mol, 75% yield based on 4,4'-oxybis(bromobenzene)). ^{1}H NMR (400 MHz, $CDCl_3$): δ 1.46 (t, 12H), 4.47 (q, 8H), 7.20 (d, 4H), 7.7 (d, 4H), 8.46 (d, 4H), 8.67 (t, 2H).

Synthesis of 4',4'''-oxybis([1,1'-biphenyl]-3,5-dicarboxylic acid) (H_4obdb):
Compound **1** (2.4 g, 0.004 mol) was dissolved in 10 mL of THF, to which 10 mL of 10 M NaOH aqueous solution was added. The mixture was stirred under reflux for 10 hours, before the organic solvent was removed using a rotary evaporator. The aqueous phase was acidified with 6M HCl to yield yellow precipitate of H_4obdb, which was filtered, washed with water, and dried under vacuum. Yield: 1.72 g, 88%. ^{1}HNMR (400 MHz, DMSO-d_6): δ, 7.22 (d, 4H), 7.81 (d, 4H), 8.38 (d, 4H), 8.45 (s, 2H), 13.38 (s, 4H).

Synthesis of FJI-H5:

$CuCl_2 \cdot 2H_2O$ (17 mg) and H_4obdb (10 mg) were dissolved in 1 mL of N,N-diethylformamide (DEF) in a 25 mL pyrex vial, to which 50 μL of HNO_3 were added. The mixture was heated in 100 ºC oven for 48 hours to yield 6 mg of blue-green crystals (yield: 46% based on H_4obdb). The crystals obtained were filtered and washed with DEF. Elemental analyses calcd (%) for $C_{84}H_{86}O_{49}Cu_6$ (After activation and absorbed small amount of water, the crystal has a formula of $Cu_6(H_2O)_6(OBDB)_3 \cdot 16H_2O$): C 44.63, H 3.83; found: C 45.62, H 3.96.

X-ray Data Collection and Structure Determination of FJI-H5:

For the single crystal analysis of **FJI-H5**, a blue-green block crystal was taken directly from the mother liquor, transferred to oil and mounted into loop. The crystal was kept at 100.00(10) K during data collection on a supernova diffractometer equipped with a Multilayers mirror Cu-Kα radiation (λ = 1.5418 Å) by using a ω scan mode. The crystal structure was solved by direct method and refined by full-matrix least squares on F^2 using *SHELXTL* package. Part of non-hydrogen atoms were refined with anisotropic displacement parameters. The free solvent molecules are highly disordered in **FJI-H5**, and attempts to locate and refine the solvent peaks were unsuccessful. The diffused electron densities resulting from these solvent molecules were removed using the *SQUEEZE* routine of *PLATON*; structures were then refined again using the data generated. Crystal data are summarized in Table S1.

Low Pressure Gas Sorption Measurements:

The N_2 adsorption/desorption isotherms were measured volumetrically using a Micromeritics ASAP 2020 surface area and pore size analyzer up to saturated pressure at 77 K. The fresh crystalline sample of **FJI-H5** was degassed under dynamic vacuum at 80 ℃ for twenty hours after solvent exchange with methanol and then dichloromethane for three days each. A color change from blue-green to deep purple-blue was observed during the activation process which is attributed to the remove of terminal coordinated water of dicopper(II) paddlewheel SBUs, thus indicating the generation of open metal sites in the framework. The specific surface areas were determined using the Brunauer-Emmett-Teller (BET) and the Langmuir equation from the N_2 sorption data. By applying the Clausius–Clapeyron equation to two sets of hydrogen adsorption data collected at 77K and 87K, the isosteric heat of adsorption ($\triangle H_{ads}$) can be obtained.

High Pressure Gas Sorption Measurements:

Gravimetric H_2 (99.999%) and CH_4 (99.999 %) adsorption measurements were performed on an HTP1-V hydrogen storage analyser (Hiden, UK) over the 0-90 bar (0-85 bar for CH_4) range at 77 K and 298 K. The total gas uptake was calculated by: $N_{total} = N_{excess} + \rho_{bulk} V_{pore}$, where ρ_{bulk} equals to the density of compressed gases at the measured temperature and V_{pore} was obtained from the N_2 isotherm at 77 K.[2]

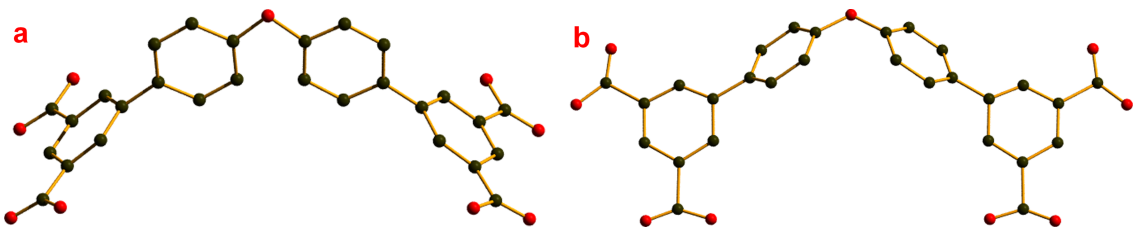

Fig. S1 Two extreme conformations of obdb ligand (black C, red O). a) the ligand in C_2 symmetry ; b) the ligand in C_s symmetry.

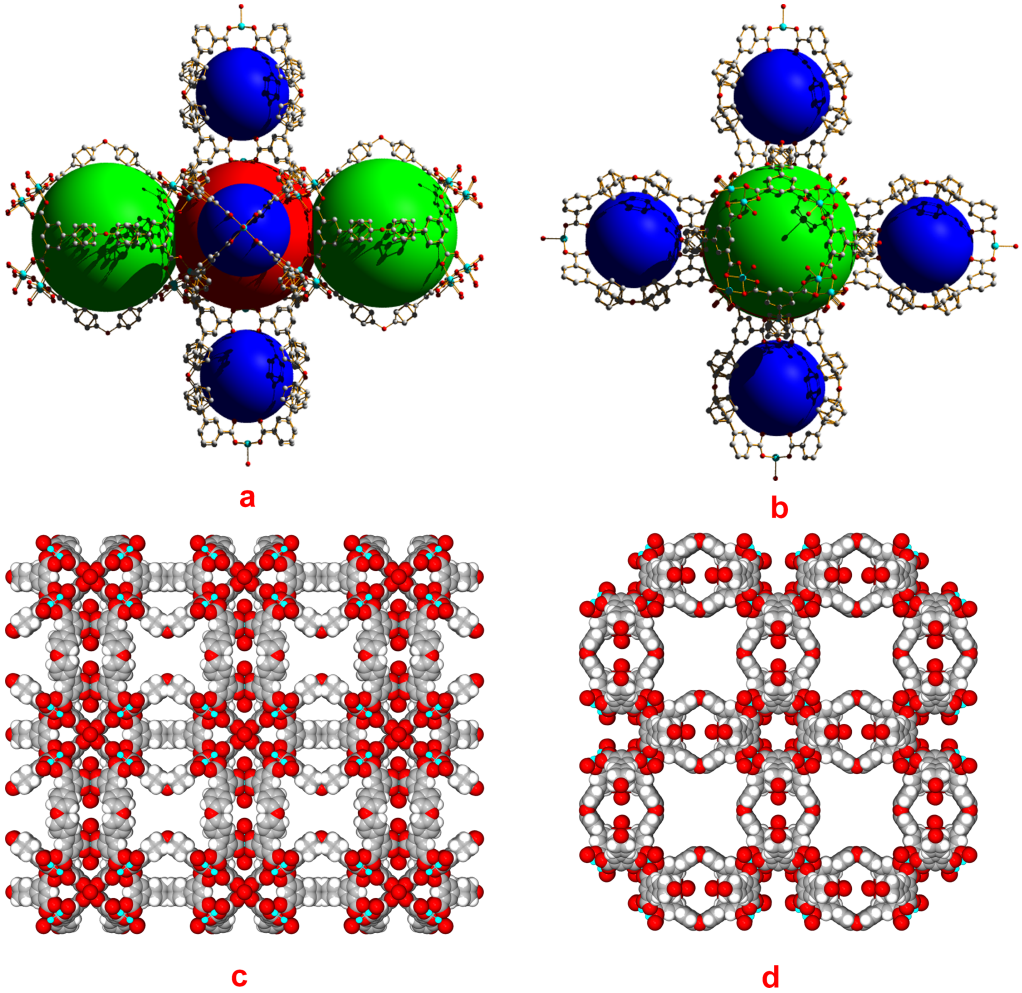

Fig. S2 a) Combination of the three types of polyhedral cages viewed along *a* axis: gray: carbon, red: oxygen, light blue: copper (colored sphere indicates pore volume, red: Cu_{24} cuboctahedral cage; green: distorted cuboctahedral cage; deep blue: compressed octahedral cage); b) Combination of the three types of polyhedral cages viewed along *c* axis; c) packing of the framework viewed along *a* axis; d) packing of the framework viewed along *c* axis.

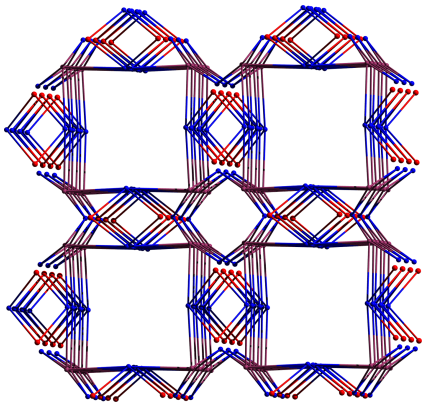

Fig. S3. Topology of **FJI-H5** simplified both obdb ligands and the Cu_2 SBUs as 4-connected nodes.

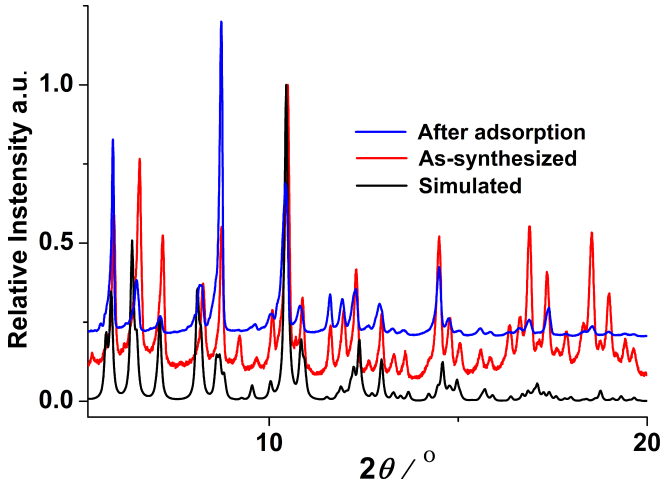

Fig. S4. Powder X-ray diffraction (PXRD) patterns of **FJI-H5**: pattern simulated from single-crystal structure in black, experimental pattern for the as-synthesized sample in red and that for the sample after adsorption in blue.

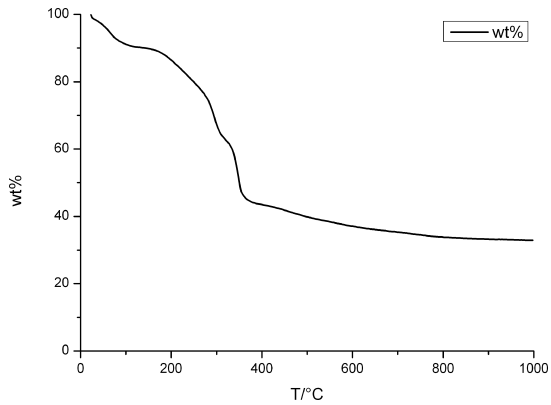

Fig. S5. TGA curves of **FJI-H5**.

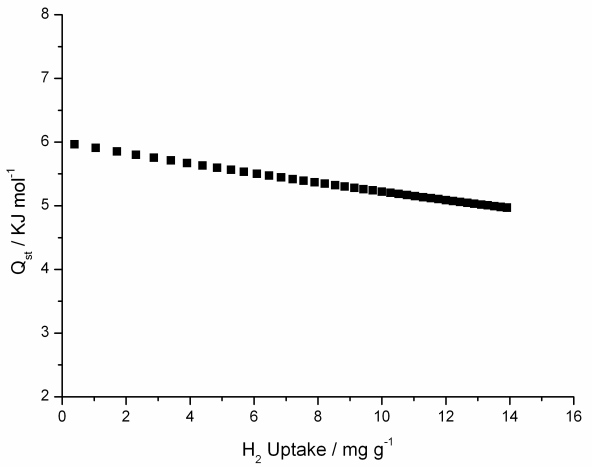

Fig. S6. Isosteric heat of H_2 adsorption at low coverage for **FJI-H5**.

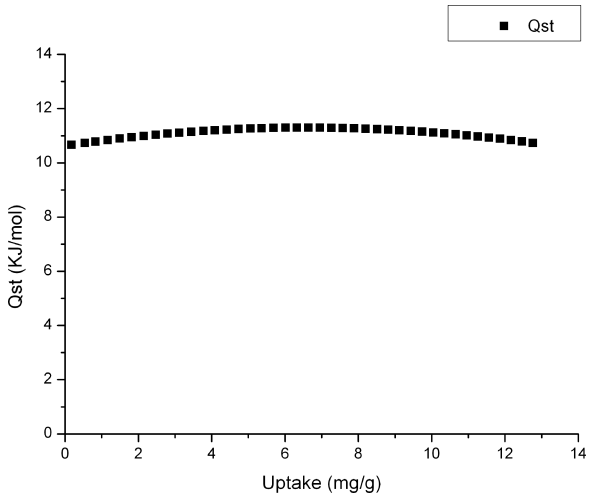

Fig. S7. Isosteric heat of CH_4 adsorption at low coverage for **FJI-H5**.

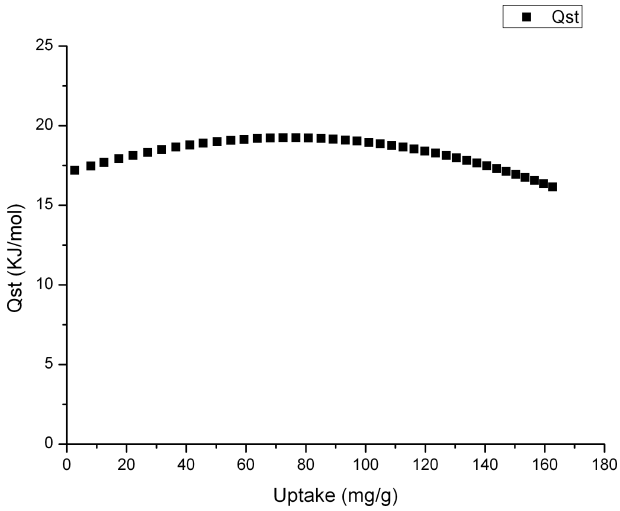

Fig. S8. Isosteric heat of CO_2 adsorption at low coverage for **FJI-H5**.

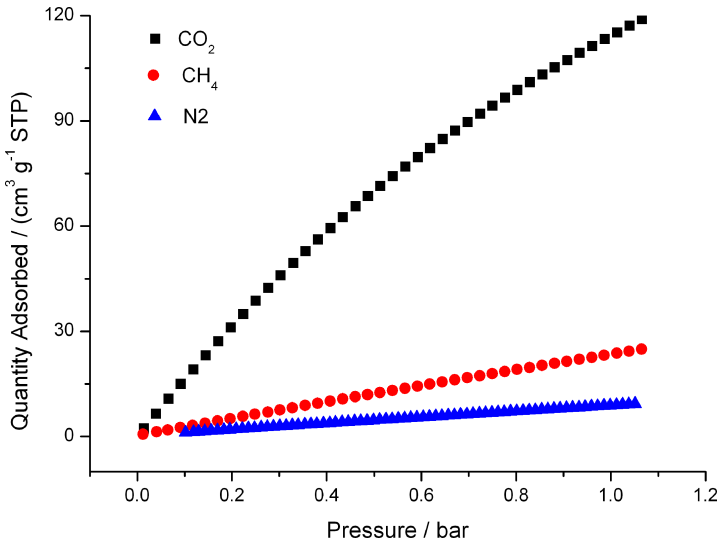

Fig. S9. Sorption isotherms for CO_2, CH_4 and N_2 at 273 K of **FJI-H5**.

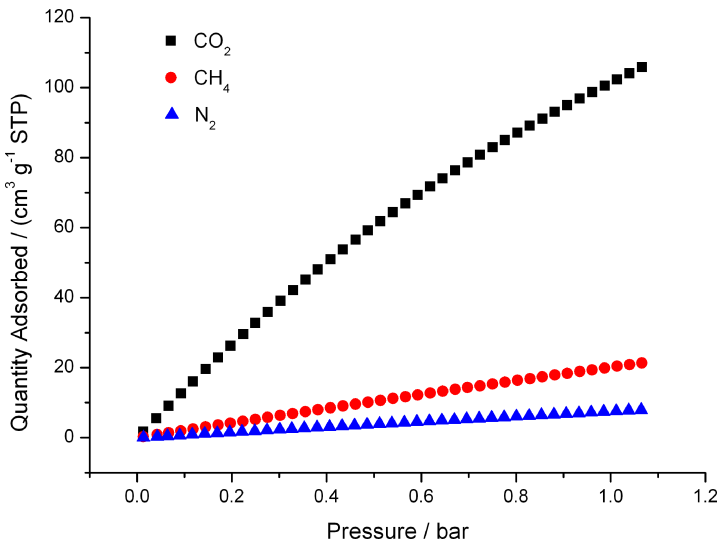

Fig. S10. Sorption isotherms for CO_2, CH_4 and N_2 at 283 K of **FJI-H5**.

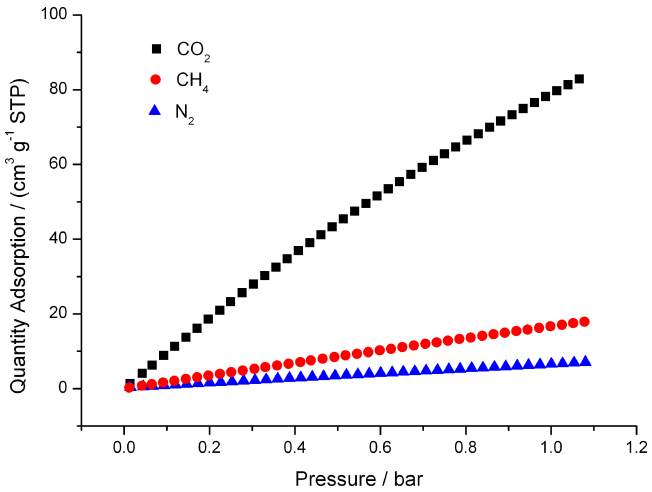

Fig. S11. Sorption isotherms for CO_2, CH_4 and N_2 at 293 K of **FJI-H5**.

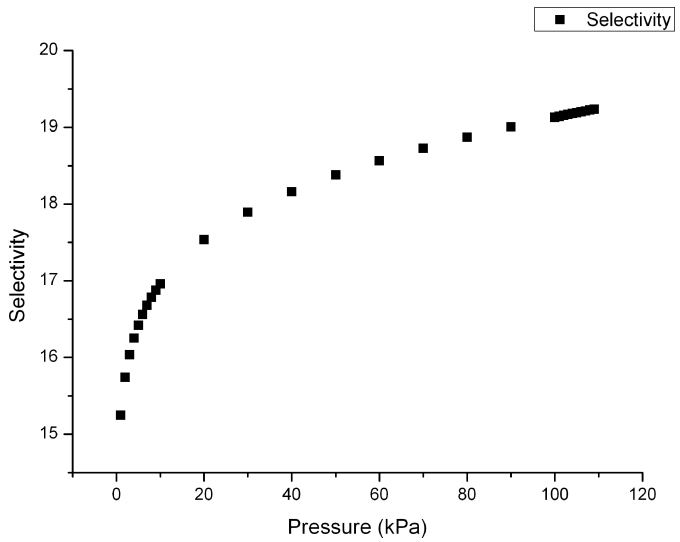

Fig. S12. IAST selectivities of CO_2 over N_2 for 15% CO_2, 85% N_2 binary mixtures in **FJI-H5** at 273 K.

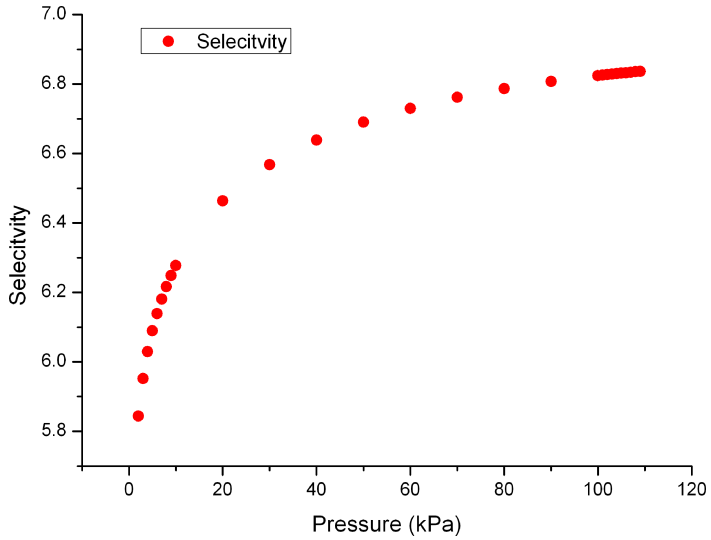

Fig. S13. IAST selectivities of CO_2 over CH_4 for equimolar binary mixtures in **FJI-H5** at 273 K.

Table S1. Crystal data and structure refinement for **FJI-H5**:

Identification code	**FJI-H5**
Empirical formula	$C_{84}H_{54}Cu_6O_{33}$
Formula weight	1972.51
Temperature	100.00(10) K
Wavelength	1.54184 Å
Crystal system	tetragonal
Space group	*P*4/*mmm*
Unit cell dimensions.	$a = b = 30.2922(13)$ Å, $c = 29.597(3)$ Å
	$\alpha = \beta = \gamma = 90$ °
Volume	27159(3) Å^3
Z	4
Density (calculated)	0.4824 mg mm^{-3}
Absorption coefficient	0.743 mm^{-1}
F(000)	3984
Crystal size	0.1×0.2×0.2 mm
θ range for data collection.	4.13 to 59.96 °
Limiting indices	$-33 <= h <= 32$, $-19 <= k <= 25$, $-33 <= l <= 32$
Reflections collected / unique	10997 / 3835 [*R*(int) = 0.1763]
Completeness	99.3 %
Absorption correction	multi-scan
Data/restraints/params	10997/59/265
Refinement method	Full-matrix least squares on F^2
Goodness of fit on F^2	1.053
Final *R* indices [*I*>2sigma(*I*)]	*R*1 = 0.1514, *wR*2 = 0.3906
R indices (all data)	*R*1 = 0.2416, *wR*2 = 0.4281

Table S2. H_2 adsorption data for selected MOFs at 1 atm and 77 K.

MOF	Gravimetric / wt %	Q_{st} / KJ mol^{-1}	Ref
PCN-12	3.05		[3]
UTSA-20	2.9		[4]
SNU-5	2.84		[5]
PCN-14	2.7	8.6	[6]
PCN-308	2.67	6.48	[7]
NOTT-110	2.64	5.68	[8]
NOTT-401	2.31	6.65	[9]
Mg-MOF-74	2.2	10.3	[10]
FJI-H5	**2.15**	**6.00**	**this work**
NOTT-400	2.14	5.96	[9]
Zn_2(BDC)(tmbd)(dabdc)(dabco)	2.08		[11]
SNU-4	2.07		[12]
FJI-1	1.02	4.62	[13]

References:

1. J. Natera, L. Otero, L. Sereno, F. Fungo, N.-S. Wang, Y.-M. Tsai, T.-Y. Hwu and K.-T. Wong, *Macromolecules*, 2007, **40**, 4456.
2. M. Dinca, a. Dailly, Y. Liiu, C. M. Brown, D. A. Neumann and j. R. Long, *J. Am. Chem. Soc.*, 2006, **128**, 16876.
3. A. Trewin and A. I. Cooper, *Angew. Chem. Int. Ed.*, 2010, **49**, 1533.
4. A. O. Yazaydin, R. Q. Snurr, T.-H. Park, K. Koh, J. Liu, M. D. Levan, A. I. Benin, P. Jakubczak, m. Lanuza, D. B. Galloway, J. J. Low and R. R. Willis, *J. Am. Chem. Soc.*, 2009, **131**, 18198.
5. L. Wen, W. Shi, X. Chen, H. Li and P. Cheng, *Eur. J. Inorg. Chem.*, 2012, **2012**, 3562.
6. A. O. Yazaydin, A. I. Benin, S. A. Faheem, P. Jakubczak, J. J. Low, R. R. Willis and R. Q. Snurr, *Chem.Mater.*, 2009, **21**, 1425.
7. Y. Liu, J. R. Li, W. M. Verdegaal, T. F. Liu and H. C. Zhou, *Chem. Eur. J.*, 2013, **19**, 5637.
8. S. Yang, X. Lin, A. Dailly, A. J. Blake, P. Hubberstey, N. R. Champness and M. Schroder, *Chem. Eur. J.*, 2009, **15**, 4829.
9. I. A. Ibarra, S. Yang, X. Lin, A. J. Blake, P. J. Rizkallah, H. Nowell, D. R. Allan, N. R. Champness, P. Hubberstey and M. Schroder, *Chem. Commun.*, 2011, **47**, 8304.
10. S. R. Caskey, A. G. Wong-Foy and A. J. Matzger, *J. Am. Chem. Soc.*, 2008, **130**, 10870.
11. H. Chun, D. N. Dybtsev, H. Kim and K. Kim, *Chem. Eur. J.*, 2005, **11**, 3521.
12. Y. G. Lee, H. R. Moon, Y. E. Cheon and M. P. Suh, *Angew. Chem. Int. Ed.*, 2008, **47**, 7741.
13. D. Han, F. L. Jiang, M. Y. Wu, L. Chen, Q. H. Chen and M. C. Hong, *Chem. Commun.*, 2011, **47**, 9861.